2010 IEEE International Conference on Robotics and Automation
Anchorage Convention District
May 3-8, 2010, Anchorage, Alaska, USA

Two-Phased Controller for a Pair of 2-DOF Soft Fingertips Based on the Qualitative Relationship between Joint Angles and Object Location

Yujiro Yamazaki, Takaihro Inoue, and Shinichi Hirai

Abstract— **We have previously shown that hemispherical soft fingertips are at equilibrium when they are in contact with objects, suggesting that the contact force and flexibility of these soft fingertips are important for stable grasping and manipulation. Hence, by making use of these characteristics, soft fingers can manipulate objects dexterously. While our previous work has focused on pairs of 1-DOF fingers with soft fingertips, we present here a control scheme by which a pair of 2-DOF soft fingers can control a grasped object's planar location. This new control scheme consists of a proportional controller of finger joint angles and an integral controller of object location. We subsequently describe our formulation of the equations of motion of manipulations performed by a pair of 2-DOF soft fingertips. We then apply this control scheme to an experimental situation and to a simulation based on a parallel distributed virtual spring model to control the planar location of a grasped object. These findings demonstrate the validity of the proposed scheme. Finally, we show that extending the theory of the proposed controller can lead to the control of grasping forces.**

I. Introduction

Soft fingertips can stably grasp objects relatively easily, because the soft material adaptively deforms along the surface of the grasped object. However, precise control is more difficult using soft than hard fingers. The phenomena in hard finger manipulation can be easily derived by kinematics. During soft finger manipulation, however, the nonlinear behavior of the soft material affects model based control. The accumulation of errors during manipulation can cause manipulation tasks to fail. In the absence of a proper model of soft fingers or a control scheme, precise manipulation cannot be realized.

Before introducing our new control scheme, we will describe the history of soft fingered robotic hands in terms of their control schemes. The first soft fingered robotic hand was proposed by Hanafusa and Asada [1], [2], who showed that the optimal prehension strategy could be derived by computing the local minimum elastic energy induced on the elastic components of soft fingers. Although they described their prehension strategy, they did not describe the manipulation that occurs after grasping an object. Use of elastic components has yielded two approaches, compliance/impedance control [3], [4], [5], [6], [7] and devices for precise assembly [8], [9]

Several realistic models of soft fingers have been proposed. For example, Akella and Cutkosky formulated a model of the contact between a soft fingertip and the surface of a rigid object to derive the dynamics of the system [10]. This model was further elaborated by adding a frictional component in analyzing the contact of soft fingertips with an object [11]. Arimoto *et al.* proposed a mathematical model in which the elastic force of a soft fingertip could be derived by solving the equations for elastic force caused by the deformation of an elastic spherical cone [12]. Using this model, they succeeded in realizing the nonlinear function of the elastic force of a soft fingertip. Based on this mathematical model, Doulgeri *et al.* proposed a feedback controller by which a pair of 2-DOF soft fingers could control an object's two coordinates and internal force [13], [14]. However, this control scheme was based on hard contact mechanism and did not include a factor for the angle dependence of soft finger elasticity, making precise control with an actual soft fingered hand difficult to accomplish. Inoue *et al.* previously described the local minimum elastic energy (LMEE), the intrinsic characteristic of a hemispherical soft fingertip [15], [16], [17]. This characteristic indicates that the induced elastic potential energy is dependent on the angle of contact with the surface, with equilibrium occurring when this angle is equal to zero. This equilibrium occurs even during soft finger manipulation, suggesting a controller that does not require a Jacobian matrix or a complicated mathematical model [18]. This controller is composed of an integral controller for generating the desired angle of the joints and a PD controller of the joint angle, allowing this controller to control the orientation of an object in the absence of a unique desired joint angle. That is, the desired angle of the finger joint is dependent on the current orientation of the object. Interestingly, the grasping force term was an independent term. Hence, by extending their theory, we hypothesized that we could design a controller that could control not only the orientation of the object, but the grasping force. Although robotic hands are thought to require 5 joints to control four DOFs of an object, by extending the controller proposed by Inoue *et al.*, we can design a controller capable of controlling three coordinates of an object and the grasping force using a pair of 2-DOF soft fingers.

This work was supported in part by JSPS Grant in Aid for Scientific Research No. 20246094.

Y. Yamazaki is with the Graduate school of Science Engineering, Robotics, Ritsumeikan University, 1-1-1 Nojihigashi, Kusatsu, Japan rr007044@ed.ritsumei.ac.jp

T. Inoue is with the Department of System Engineering for Sports, Okayama Prefectural University, Japan inoue@ss.oka-pu.ac.jp

S. Hirai is with the Faculty of the Department of Robotics, Ritsumeikan University, Japan hirai@se.ritsumei.ac.jp

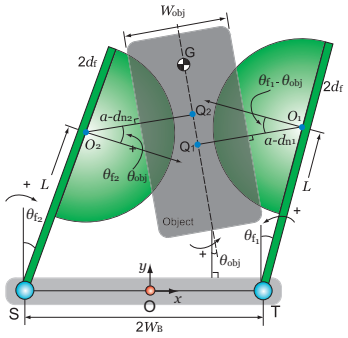

Fig. 1. A pair of 1-DOF fingers with soft fingertips

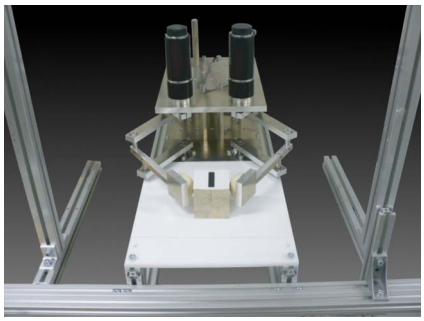

Fig. 2. A pair of 2-DOF soft fingered robotic hands

We describe here a new controller by which a soft fingered hand can control an object's three coordinates. We explain the dynamic model of a pair of 2-DOF soft fingers. We assess the validity of this controller by applying it to an actual soft fingered hand. Finally, we show that the grasping force can be controlled by introducing feedback to the proposed controller.

II. Two-Phased Object Location Controller

In this section, we introduce a new control scheme for a two 2-DOF soft fingered robotic hand based on a two-phased object orientation controller.

A. Two Phased Object Orientation Controller

The softness of a soft fingertip is a major factor in object manipulation. In hard fingered manipulation, all joints of a robotic hand must be computed using inverse kinematics. In soft fingered manipulation, however, the soft material adaptively deforms against the surface of an object. Consequently, even if it was imprecisely controlled, the grasped state can be maintained. Failure of a model-based controller is therefore due to the unexpected behavior of the soft fingertips. In contrast, a control without a Jacobian matrix is effective for soft fingered manipulation. In describing a two phased orientation controller, Inoue *et al.* showed that the contact state of a soft finger and object always converges to the local minimum elastic energy with constraints (LMEEwC) in manipulation; they also introduced a controller without a Jacobian matrix, which gradually generates the desired angle of rotational finger joint from the LMEEwC state.

Fig. 1 shows a rigid object grasped by a pair of 1-DOF fingers with soft fingertips. Assume that a vision system can measure the orientation of the grasped object. The issue to be tackled was to build a controller that regulates the orientation of an object $\theta_{\rm obj}$ to its desired value $\theta^{\rm d}_{\rm obj}$ by controlling the right finger angle θ_{f1} and the left finger angle θ_{f2}. Using this newly designed controller, Inoue *et al.* succeeded in controlling a grasped object's orientation. Their controller consists of two phases: the first for generating virtual desired angles and the second for following the virtual desired angles. In the first phase, the virtual desired angles for the right and left fingers can be computed as:

$$\theta^{\rm d}_{f1} = K_I \int_0^t (\theta_{\rm obj} - \theta^{\rm d}_{\rm obj})\,{\rm d}\tau, \tag{1}$$

$$\theta^{\rm d}_{f2} = -K_I \int_0^t (\theta_{\rm obj} - \theta^{\rm d}_{\rm obj})\,{\rm d}\tau. \tag{2}$$

These equations are due to the nature of the object grasped by a pair of 1-DOF fingers with soft tips. When two fingers rotate counter clockwise, the object rotates clockwise. This indicates that, when θ_{f1} (the angle of the right finger) increases and θ_{f2} (the angle of the left finger) decreases, $\theta_{\rm obj}$ decreases. Thus, when $\theta_{\rm obj} > \theta^{\rm d}_{\rm obj}$, we would increase θ_{f1} and decrease θ_{f2} to rotate the object clockwise. Thus, when $\theta_{\rm obj} > \theta^{\rm d}_{\rm obj}$, $\theta^{\rm d}_{f1}$ increases and $\theta^{\rm d}_{f2}$ decreases. In contrast, when $\theta_{\rm obj} < \theta^{\rm d}_{\rm obj}$ $\theta^{\rm d}_{f1}$ decreases and $\theta^{\rm d}_{f2}$ decreases. Consequently, the above equations are based on the qualitative relationship between joint angles (θ_{f1} and θ_{f2}) and object angle. The second phase applies a simple PD control law to follow the virtual desired angles:

$$u_i = -K_P(\theta_{fi} - \theta^{\rm d}_{fi}) - K_D\dot{\theta}_{fi} + f_{\rm const}, \quad (i = 1,2), \tag{3}$$

where u_i denotes the input torque applied to the i-th finger joint and $f_{\rm const}$ denotes a constant torque to generate grasping forces at the both fingers. During the second phase, the joint angles do not have to track their virtual desired angles; hence, the PD control law is applied instead of the PID control law. As mentioned above, their controller does not require a Jacobian matrix. That is, because this controller was made using a simplified motion relationship between soft fingers and grasped objects. For example, when two fingers rotate counter clockwise, the object rotates clockwise.

In describing the qualitative relationship between object orientation and joint angles, an increase can be denoted by the symbol $\uparrow$ and a decrease by the symbol $\downarrow$. The above relationship can then be described as:

$$\theta_{\rm obj}\downarrow \quad : \quad \theta_{f1}\uparrow, \quad \theta_{f2}\downarrow \tag{4}$$

Note that the sign in eq. (1) is positive when $\theta_{f1}\uparrow$ is satisfied and the sign in eq. (2) is negative when $\theta_{f2}\downarrow$ is satisfied. Consequently, the qualitative relationship determines the sign of the integral controller in the first phase.

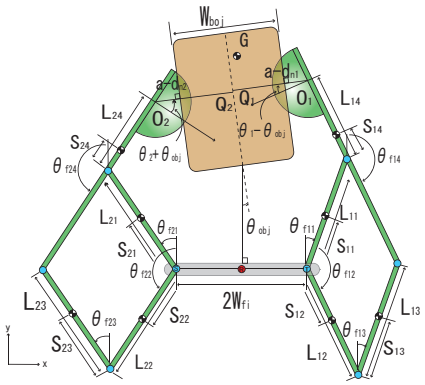

Fig. 3. A model of the robotic hand

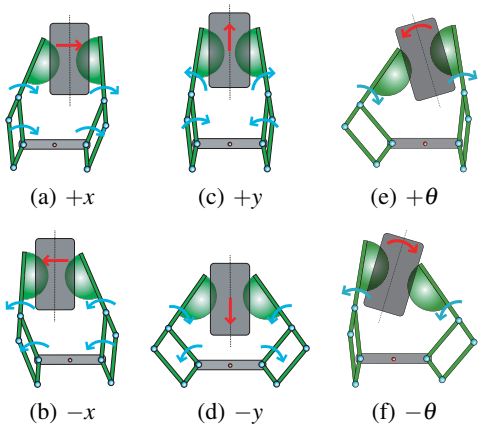

Fig. 4. Motion Relationship

B. Extension to Two Phased Object Location Controller

The soft fingered hand mentioned in this paper is shown in Fig. 2. A model of the hand is shown in Fig. 3. Let the right finger seen from the hand side be the first finger and the left finger be the second finger. Let $(x_{\rm obj}, y_{\rm obj})$ be the position of a grasped object, $\theta_{\rm obj}$ be that of the tilt, a be the radius of the soft fingertips, d_{ni} be the deformation of the i-th fingertip which is perpendicular to the surface of the object, and $W_{\rm obj}$ be the width of the object. Let $2W_{fi}$ be the distance of the base coordinates of two soft fingers, w be the distance between the center of the object and COG in the normal direction and L_{ij} be the length of the i-th finger's j-th link. Thus, subscript i represents the i-th finger and subscript j represents the j-th link. Let θ_{ij} be each joint angle. The positive rotation of the first finger is therefore counter clockwise, and the positive rotation of the second finger is clockwise. Let $2d_{fi}$ be the thickness of the links of the fingers.

The new control scheme is aimed at controlling a grasped object's two translational positions, one orientation in the 2D plane without the force of gravity. We sought to build a controller that regulates the position of the object $(x_{\rm obj}, y_{\rm obj})$ to its desired value $(x^{\rm d}_{\rm obj}, y^{\rm d}_{\rm obj})$ and the orientation of the object $\theta_{\rm obj}$ to its desired value $\theta^{\rm d}_{\rm obj}$ by controlling the angles of the right finger θ_{11} and θ_{12} and left finger θ_{21} and θ_{22}. The basic idea of the new control scheme was identical to that of the previous control scheme. The new control scheme controller has two phases, the first producing the desired joint angle and the second controlling the finger with a simple PD controller. However, a higher degree of freedom of manipulation is needed to extend this idea. To enable a higher degree of freedom, it is essential to introduce another two integral controllers to produce the desired angle of each joint. We therefore introduced these three integral controllers:

$$I^{\rm d}_x = K_{Ix} \int_0^t (x_{\rm obj} - x^{\rm d}_{\rm obj})\, {\rm d}\tau, \tag{5}$$

$$I^{\rm d}_y = K_{Iy} \int_0^t (y_{\rm obj} - y^{\rm d}_{\rm obj})\, {\rm d}\tau, \tag{6}$$

$$I^{\rm d}_\theta = K_{I\theta} \int_0^t (\theta_{\rm obj} - \theta^{\rm d}_{\rm obj})\, {\rm d}\tau. \tag{7}$$

In addition, the structure of the controller must be changed to subsume the simplified motion relationship of the soft fingers and grasped object seen in the manipulation. In the equation, u_{ij} denotes the input for the respective rotational joints. To enable two translational and one rotational motions, these simplified motion relationships should be divided into six states, as shown in Fig. 4. The relationship can be explained using one example. As shown in Fig. 4-(c), increasing u_{11} and u_{21} while decreasing u_{12} and u_{22} makes the object move upward. This indicates that, if $y_{\rm obj}$ is less than $y^{\rm d}_{\rm obj}$, u_{11} and u_{21} should be increased while u_{12} and u_{22} should be decreased. In describing the qualitative relationship between object position/orientation and joint angles, we found that Fig. 4 yields the relationships:

$$x_{\rm obj}\downarrow \ : \ \theta_{11}\uparrow, \quad \theta_{21}\downarrow, \quad \theta_{12}\uparrow, \quad \theta_{22}\downarrow, \tag{8}$$

$$y_{\rm obj}\downarrow \ : \ \theta_{11}\downarrow, \quad \theta_{21}\downarrow, \quad \theta_{12}\uparrow, \quad \theta_{22}\uparrow, \tag{9}$$

$$\theta_{\rm obj}\downarrow \ : \ \theta_{12}\uparrow, \quad \theta_{22}\downarrow. \tag{10}$$

An increase is denoted by a positive sign, and a decrease by a negative sign. The virtual desired values can then be expressed as:

$$\begin{aligned} \theta^x_{11} &= \ I_x, \quad \theta^y_{11} = -I_y, \\ \theta^x_{21} &= -I_x, \quad \theta^y_{21} = -I_y, \\ \theta^x_{12} &= \ I_x, \quad \theta^y_{12} = \ I_y, \quad \theta^\theta_{12} = \ I_\theta, \\ \theta^x_{22} &= -I_x, \quad \theta^y_{22} = \ I_y, \quad \theta^\theta_{22} = -I_\theta. \end{aligned}$$

In applying PD controllers so that joint angles follow their desired values, there are now three variables to be regulated; $x_{\rm obj}$, $y_{\rm obj}$, and $\theta_{\rm obj}$. After taking the sum of the three PD controllers for each joint angle, the new control scheme can be expressed as

$$\begin{aligned} u_{i1} = &-K_{Px}(\theta_{i1} - \theta_{i1(0)} - \theta^x_{i1}) - K_{Dx}\dot{\theta}_{i1} \\ &-K_{Py}(\theta_{i1} - \theta_{i1(0)} - \theta^y_{i1}) - K_{Dy}\dot{\theta}_{i1} + f_{\rm const} \end{aligned} \tag{11}$$

$$\begin{aligned} u_{i2} = &-K_{Px}(\theta_{i2} - \theta_{i2(0)} - \theta^x_{i2}) - K_{Dx}\dot{\theta}_{i2} \\ &-K_{Py}(\theta_{i2} - \theta_{i2(0)} - \theta^y_{i2}) - K_{Dy}\dot{\theta}_{i2} \\ &-K_{P\theta}(\theta_{i2} - \theta_{i2(0)} - \theta^\theta_{i2}) - K_{D\theta}\dot{\theta}_{i2} + f_{\rm const} \end{aligned} \tag{12}$$

In the newly proposed controller (Fig. 4), all rotational joints play a role in controlling the two axial translational position of the grasped object. In contrast, only the upper two rotational joints play a role in controlling the orientation of the object. Since the parallel link mechanism has a singular point, the joint angles may be limited. The initial angle of each joint was not zero, such that the incipient inputs may be extremely high. To eliminate any incipient inputs that are too high, we added the term $\theta_{ij(0)}$ which denotes the initial angle of each joint in the controllers.

III. Equations of Motion of Two-Fingered Hand with Soft Fingertips

In this section, we derive the equations of motion for object manipulations performed by two 2-DOF robotic fingers with soft fingertips driven by a parallel link mechanism (Fig. 3). Since the area of manipulation was limited to a 2D plane, the influence of a gravitational potential energy term can be ignored. We employed a parallel distributed model [16], [17], which includes not only a nonlinear function of soft fingertip elasticity but also an angle dependent elasticity function. Since we supposed that the two soft fingers and the grasped object form a closed link mechanism without any slippage between the soft fingertips and the object, we introduced four geometric constraints, two holonomic constraints that generate normal constraints on the object surface and fingertips, and two nonholonomic constraints that generate tangential constraints on the object and fingertips. In this section, we start by explaining the four constraints. We next describe the parallel distributed model, kinetic energy and equations of motion. Finally, we introduce a numerical solution that simulates soft fingered manipulations.

A. Holonomic and Nonholonomic Constraints

In formulating the geometric constraints imposed on each fingertip, the position of the center of the i-th fingertip can be expressed as

$$\begin{aligned} O_{ix} =&(-1)^{i+1}W_{fi}+(-1)^{i}L_{i1}\sin\theta_{i1} \\ &+(-1)^{i}L_{i4}\sin(\theta_{i2}-\pi)+(-1)^{i}d_{fi}\cos(\theta_{i2}-\pi), \quad (13) \\ O_{iy} =&L_{i1}\cos\theta_{i1}+L_{i4}\cos(\theta_{i2}-\pi) \\ &-d_{fi}\sin(\theta_{i2}-\pi). \quad (14) \end{aligned}$$

The two holonomic constraints can be represented by the geometric relationship of the i-th fingertip and the surface of the object as:

$$\begin{aligned} C_i^H =&(-1)^{i}(x_{\rm obj}-O_{ix})\cos\theta_{\rm obj} \\ &+(-1)^{i}(y_{\rm obj}-O_{iy})\sin\theta_{\rm obj} \\ &-(a-d_{ni})+\frac{W_{\rm obj}}{2}+(-1)^{i}w=0. \quad (15) \end{aligned}$$

In contrast, the tangential constraints depend on the trajectory and are therefore represented as nonholonomic constraints. As mentioned above, if each inward finger rotation is positive, the rolling speed of the object can be expressed as

$$\dot{s}_i=-(a-d_{ni})\{\dot{\theta}_{i2}+(-1)^{i}\dot{\theta}_{\rm obj}\}. \quad (16)$$

In addition, the distance of GQ_i can be expressed as

$$GQ_i=-(x_{\rm obj}-O_{ix})\sin\theta_{\rm obj}+(y_{\rm obj}-O_{iy})\cos\theta_{\rm obj}, \quad (17)$$

as shown in Fig. 3. Let d_{ti} be the tangential deformation of the i-th soft fingertip, which is parallel to the surface of the object. Using equation (16), we can calculate the relative velocity between the object and the center of the fingertip by differentiating the GQ_i. Finally, we can determine the nonholonomic constraints, called Pfaffian constraints, using the equation:

$$C_i^N=\dot{GQ}_i-\dot{s}_i+\dot{d}_{ti}. \quad (18)$$

Finally, we can calculate the four constraints.

B. Two-dimensional Model of Soft Fingertips

To derive the lagrangian, we must first derive the elastic potential energy of soft fingertips. The relative angle between an object and a soft finger θ_{pi} can be expressed as

$$\theta_{pi}=\theta_{i2}-\pi+(-1)^{i}\theta_{\rm obj}. \quad (19)$$

According to [16], the elastic potential energy determined by the parallel distributed model can be expressed as

$$P_{fi}=\pi E\left\{\frac{d_n^3}{3\cos^2\theta_{pi}}+d_{ni}^2d_{ti}\tan\theta_{pi}+d_{ni}d_{ti}^2\right\}, \quad (20)$$

where E denotes Young's modulus of the material of the soft fingertip. If θ_{pi} is the relative angle between the object and the fingertip, we can calculate the entire elastic potential energy as

$$P_i=\pi E\sum_{i=1}^{2}\left\{\frac{d_n^3}{3\cos^2\theta_{pi}}+d_{ni}^2d_{ti}\tan\theta_{pi}+d_{ni}d_{ti}^2\right\}. \quad (21)$$

C. Lagrangian

The lagrangian can be derived from the kinetic energy, elastic potential energy and constraints. We therefore must formulate the kinetic energy in this soft fingered manipulation. The kinetic energy of the two 2-DOF soft fingered hand shown in Fig. 3 can be expressed as a pair of parallel link mechanism manipulators. If S_{ij} is the distance between the rotational joint and the center of gravity of each link, the position of each link can be expressed as

$$\begin{aligned} x_{i1}&=(-1)^{i+1}W_{fi}+(-1)^{i}S_{i1}\sin\theta_{i1}, \\ y_{i1}&=S_{i1}\cos\theta_{i1}, \\ x_{i2}&=(-1)^{i+1}W_{fi}+(-1)^{i}S_{i2}\sin\theta_{i2}, \\ y_{i2}&=S_{i2}\cos\theta_{i2}, \\ x_{i3}&=(-1)^{i+1}W_{fi}+(-1)^{i}L_{i2}\sin\theta_{i2}+(-1)^{i}S_{i3}\sin\theta_{i1}, \\ y_{i3}&=L_{i2}\cos\theta_{i2}+S_{i3}\cos\theta_{i1}, \\ x_{i4}&=(-1)^{i+1}W_{fi}+(-1)^{i}L_{i1}\sin\theta_{i1}+(-1)^{i}S_{i4}\sin(\theta_{i2}-\pi), \\ y_{i4}&=L_{i1}\cos\theta_{i1}+S_{i4}\cos(\theta_{i2}-\pi). \end{aligned}$$

Consequently, the kinetic energy of two soft fingers with a parallel link mechanism and a grasped object can be

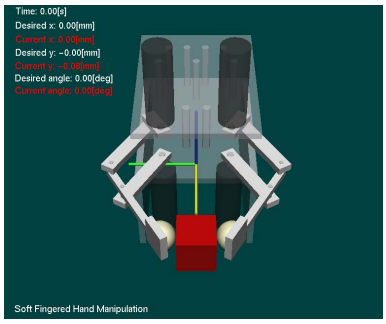

Fig. 5. Snapshot of simulation

represented as

$$K = \sum_{i=1}^{2}\sum_{j=1}^{4}\frac{1}{2}m_{ij}(\dot{x}_{ij}^2+\dot{y}_{ij}^2)+\sum_{i=1}^{2}\sum_{j=1}^{4}\frac{1}{2}I_{ij}\dot{\theta}_{ij}^2 + \frac{1}{2}m_{\mathrm{obj}}(\dot{x}_{\mathrm{obj}}^2+\dot{y}_{\mathrm{obj}}^2)+\frac{1}{2}I_{\mathrm{obj}}\dot{\theta}_{\mathrm{obj}}^2 \tag{22}$$

where m_{ij} is the mass and I_{ij} is the moment of inertia of each link. It should be emphasized that angle θ_{ij} can be represented as four joint angles θ_{11}, θ_{12}, θ_{21} and θ_{22}, so θ_{i3} and θ_{i4} can be replaced by θ_{i1} and θ_{i2} respectively.

It is also necessary to add the holonomic constraint related term to the lagrangian. This term can be represented using Lagrange's multiplier and formula of constraint. Finally, we can calculate the lagrangian as:

$$L = K - P + \sum_{i=1}^{2}\lambda_i^H C_i^H, \tag{23}$$

where λ_1^H and λ_2^H represent Lagrange multipliers corresponding to holonomic constraints C_1^H and C_2^H respectively. Vector $\boldsymbol{\lambda}^N = [\lambda_1^H, \lambda_2^H]^{\mathrm{T}}$ is referred to as the holonomic constraint force vector.

D. Equations of Motion

If $\boldsymbol{q}$ is an 11-dimensional vector consisting of the generalized variables, x_{obj}, y_{obj}, θ_{obj}, θ_{11}, θ_{12}, θ_{21}, θ_{22}, d_{n1}, d_{n2}, d_{t1}, and d_{t2}, then, by adding the nonholonomic constraints, we can obtain the following equations of motion for soft fingered manipulation:

$$\frac{d}{dt}\frac{\partial L}{\partial \dot{\boldsymbol{q}}} - \frac{\partial L}{\partial \boldsymbol{q}} = \boldsymbol{\Phi}^{NT}\boldsymbol{\lambda}^N \in R^{11\times 1}. \tag{24}$$

The term $\boldsymbol{\Phi}^{NT}$ can be defined as a partially differentiated constraint matrix of nonholonomic constraints. Each element of this matrix can be expressed as

$$\left(\boldsymbol{\Phi}^{NT}\right)_{i,j} = \frac{\partial C_i^N}{\partial \dot{q}_j}. \tag{25}$$

In addition, the equation $\boldsymbol{\lambda}^N = [\lambda_1^N, \lambda_2^N]^{\mathrm{T}}$ can represent the nonholonomic constraint force vector applied along the surface of the object. That is, the nonholonomic constraint force vector is a vector composed of Lagrange's multipliers.

E. Simulation using Constraint Stabilization Method

The Constraint Stabilization Method (CSM) is a numerical method for solving ordinary differential equations under geometric constraints. We have used this method to make the constraints applicable to the two holonomic and two nonholonomic constraints. The CSM equations for holonomic and nonholonomic constraints can be expressed as

$$\ddot{\boldsymbol{C}}^H + 2\alpha\dot{\boldsymbol{C}}^H + \alpha^2\boldsymbol{C}^H = 0 \in R^{2\times 1}, \tag{26}$$

$$\dot{\boldsymbol{C}}^N + \beta\boldsymbol{C}^N = 0 \in R^{2\times 1}, \tag{27}$$

where α and β denote the CSM parameters. The higher these parameters, the faster the deviation of constraints converge to zero. Let $\dot{\boldsymbol{C}}^H$ and $\dot{\boldsymbol{C}}^N$ be vectors composed of holonomic constraints given in (15) and Pfaffian constraints given in (18), respectively. For convenience of simulation, (26) and (27) can be represented as

$$\boldsymbol{\Phi}^H\dot{\boldsymbol{p}} = -\boldsymbol{b}^H(\boldsymbol{q},\boldsymbol{p}) - 2\alpha\dot{\boldsymbol{C}}^H - \alpha^2\boldsymbol{C}^H \triangleq -\boldsymbol{\gamma}^H \tag{28}$$

$$\boldsymbol{\Phi}^N\dot{\boldsymbol{p}} = -\boldsymbol{b}^N(\boldsymbol{q},\boldsymbol{p}) - \beta\boldsymbol{C}^N \triangleq -\boldsymbol{\gamma}^N, \tag{29}$$

where $\boldsymbol{p}$ is the velocity vector, the time derivative of $\boldsymbol{q}$. If $\boldsymbol{\Phi}^N$ represents the partially differentiated holonomic constraints, then each component of vector $\boldsymbol{\Phi}^N$ will correspond to

$$\Phi_{ij}^H = \frac{\partial C_i^H}{\partial q_j}, \qquad (i=1,2 : j=1,2,\ldots,11). \tag{30}$$

If $\boldsymbol{f}_p$ is the potential force vector, $\boldsymbol{f}_{ext}$ is the external force vector, and $\boldsymbol{u}_{IN}$ is the input vector for each rotational joint, then the equations of motion can be expressed simply as:

$$\begin{bmatrix} \boldsymbol{I} & \boldsymbol{0} & \boldsymbol{0} & \boldsymbol{0} \\ \boldsymbol{0} & \boldsymbol{M} & -\boldsymbol{\Phi}^{HT} & -\boldsymbol{\Phi}^{NT} \\ \boldsymbol{0} & -\boldsymbol{\Phi}^H & \boldsymbol{0} & \boldsymbol{0} \\ \boldsymbol{0} & -\boldsymbol{\Phi}^N & \boldsymbol{0} & \boldsymbol{0} \end{bmatrix}\begin{bmatrix} \dot{\boldsymbol{q}} \\ \dot{\boldsymbol{p}} \\ \boldsymbol{\lambda}^H \\ \boldsymbol{\lambda}^N \end{bmatrix} = \begin{bmatrix} \boldsymbol{p} \\ -\boldsymbol{f}_p + \boldsymbol{f}_{ext} + \boldsymbol{u}_{IN} \\ \boldsymbol{\gamma}^H \\ \boldsymbol{\gamma}^N \end{bmatrix}. \tag{31}$$

This matrix includes CSM equations and equations of motion. By numerically integrating those equations, we can observe the manipulation performed by a soft fingered hand with parallel link mechanism. The constructed simulation is shown in Fig. 5.

IV. Simulation of Object Location Control

We simulated a manipulation performed by a pair of 2-DOF soft fingered hands, without including the effect of the force of gravity, to determine the validity of our proposed control scheme. In the simulation, both position control and orientation control were simulated. Physical parameters, parameters of simulation and control gains are shown in Tables I, II and III, respectively. All the parameters in Table I are based on an actual soft fingered hand. If the point of origin is the initial position of the grasped object, the sequence of control can be represented as shown in Table IV.

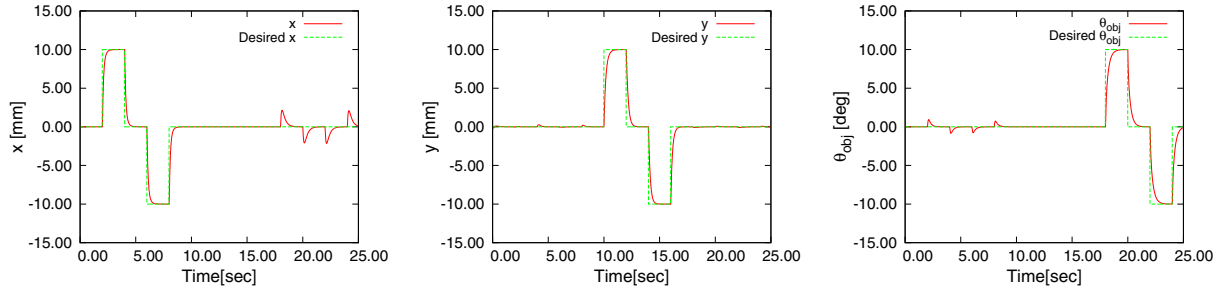

(a) x_{obj} vs. time (b) y_{obj} vs. time (c) θ_{obj} vs. time

Fig. 6. Simulation result of object position and orientation control

TABLE I

PHYSICAL PARAMETERS

Parameters	Value
m_{obj}	0.1 kg
I_{obj}	41.7 kg·mm^2
W_{obj}	50 mm
$2W_{fi}$	100 mm
d_{fi}	5 mm
$L_{11}, L_{21}, L_{13}, L_{23}, L_{14}, L_{24}$	100 mm
L_{12}, L_{22}	30 mm
S_{11}, S_{21}	4.9 mm
S_{12}, S_{22}	1.4 mm
S_{13}, S_{23}	4.5 mm
S_{14}, S_{24}	5.7 mm
m_{11}, m_{21}	66 g
m_{12}, m_{22}	28 g
m_{13}, m_{23}	73 g
m_{14}, m_{24}	113 g
I_{11}, I_{21}	224.5 kg·mm^2
I_{12}, I_{22}	13.6 kg·mm^2
I_{13}, I_{23}	233.5 kg·mm^2
I_{14}, I_{24}	672.7 kg·mm^2
Viscosity for d_{ni}	400Ns/m
Viscosity for d_{ti}	400Ns/m
E Young's modulus	0.232MPa

TABLE II

PARAMETERS OF SIMULATION

Parameters	Value
Sampling time	0.1 ms
α	20000
β	10000

Simulation results are shown in Fig. 6. These three graphs show that the simulation results converge to the desired position or orientation. As shown by Inoue *et al*, the contact state converges to an equilibrium uniquely dependent on the positions of the fingertips and the object. Furthermore, the joint angle of two fingers adapts to match the current coordinates of the grasped object with the desired coordinates. Consequently, the non-Jacobian controller can precisely control the object coordinates by adapting the finger joint angles based on the LMEEwC. These findings show the validity of the proposed controller in controlling object planar coordinates.

TABLE III

CONTROL GAINS

Parameters	Value
Sampling time of object coordinates data	30 ms
K_{Px} gain	70
K_{Py} gain	70
$K_{P\theta}$ gain	20
K_{Dx} gain	20
K_{Dy} gain	20
$K_{D\theta}$ gain	20
K_{Ix} gain	0.1
K_{Iy} gain	0.1
$K_{I\theta}$ gain	0.02
f_{const}	2 Nm

TABLE IV

SEQUENCE OF DESIRED POSITION AND ORIENTATION

operation	$x^{\mathrm{d}}_{\mathrm{obj}}$ (mm)	$y^{\mathrm{d}}_{\mathrm{obj}}$ (mm)	$\theta^{\mathrm{d}}_{\mathrm{obj}}$ (deg)
#1	10	0	0
#2	0	0	0
#3	−10	0	0
#4	0	0	0
#5	0	10	0
#6	0	0	0
#7	0	−10	0
#8	0	0	0
#9	0	0	10
#10	0	0	0
#11	0	0	−10

V. EXPERIMENT OF OBJECT LOCATION CONTROL

The same manipulation was performed by an actual soft fingered hand. Gains of the controller were set as in Table II. The control order was the same as for the simulation. The results of this experiment are shown in Fig. 7. As with the simulation, we observed the convergence of the results to the desired values. Vibrations can be seen in the results. However, the convergences were faster during actual than during simulated manipulation. Thus, in actual soft fingered manipulation, our proposed controller can work precisely.

VI. SIMULATION OF OBJECT FORCE AND LOCATION CONTROL

In daily life, we must manipulate various kinds of objects, with some being rigid, some fragile, and some having complex shapes. In our manipulations of these objects, we

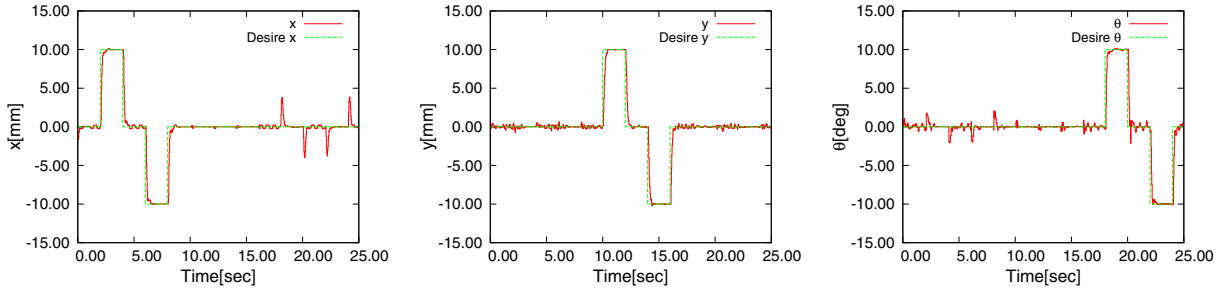

(a) x_{obj} vs. time (b) y_{obj} vs. time (c) θ_{obj} vs. time

Fig. 7. Experimental results of object location control

only vaguely consider these mechanical components, and we must use and control our soft fingered hands under these circumstances. In this section, we propose the possible design of a grasping force controller, and we manipulate a trapezoidal prism to show that the proposed controller can be used for various kinds of objects.

Before introducing the new controller, it is necessary to extend the simulation model to include the manipulation of a trapezoidal prism. The mathematical model can be extended simply by altering the constraints equations (15), (17), and the relative angle of elastic potential energy (21):

$$\begin{aligned} C_i^H =&(-1)^i(x_{\text{obj}}-O_{ix})\cos(\theta_{\text{obj}}+(-1)^i\psi_i)\\ &+(-1)^i(y_{\text{obj}}-O_{iy})\sin(\theta_{\text{obj}}+(-1)^i\psi_i)\\ &-(a-d_{ni})+\frac{W_{iobj}}{2}+(-1)^i w=0, \end{aligned} \tag{32}$$

$$\begin{aligned} GQ_i =&-(x_{\text{obj}}-O_{ix})\sin(\theta_{\text{obj}}+(-1)^i\psi_i)\\ &+(y_{\text{obj}}-O_{iy})\cos(\theta_{\text{obj}}+(-1)^i\psi_i), \end{aligned} \tag{33}$$

$$\theta_{pi}=\theta_{i2}-\pi+(-1)^i\theta_{\text{obj}}-(-1)^i\psi_i. \tag{34}$$

If ψ_i is the angle of the object's surface on the side of the i-th finger and W_{iobj} is the thickness of the object on the side of the i-th finger, then the remaining derivation is identical to that for the manipulation of a cube.

Our controller was found to be an independent controller of grasping force, indicating that control of grasping force control occurs simultaneously with control of object coordinates. To determine whether this was so, we attempted to control grasping force and coordinates simultaneously by introducing a grasping force controller to an object location controller. Attaching a force sensor to the back of the fixed end of a right finger's soft fingertip can enable measurement of the grasping force of that hand. If f_{v1} is the grasping force acting from the fixed end of a soft fingertip and f_{v1}^{d} is its desired value, the new controller can be expressed by replacing the f_{const} terms of (11) and (12) with f_{grasp} below:

$$\theta_{ij}^f=-K_{If}\int_0^t(f_{v1}-f_{v1}^{\text{d}})\,\text{d}\tau, \tag{35}$$

$$f_{\text{grasp}}=-K_{Pf}\left\{\theta_{ij}-\theta_{ij(0)}-\theta_{ij}^f\right\}-K_{Df}\dot{\theta_{ij}}. \tag{36}$$

TABLE V
FORCE CONTROL GAINS

Parameters	Value
K_{Pf} gain	70
K_{Df} gain	0
K_{If} gain	0.1

These equations again denote the first and second phases of the controller.

In this simulation, we used the Lagrange multiplier of holonomic constraints for force feedback. This multiplier corresponds to the normal reaction force on the surface of an object. The parameters are identical to those in the previous simulation. The parameters of the grasping force controller are shown in Table V. The control sequence was identical to that of the previous simulation, with $f_{v1}^{\text{d}}=2$ N, but there were two additional operations, where the object should remain in zero location with $f_{v1}^{\text{d}}=1$ N and $f_{v1}^{\text{d}}=3$ N in sequence.

The results of simulation are shown in Fig. 8. Compared with the previous simulation, there were no differences in x_{obj}, y_{obj} and θ_{obj}. We also observed that the result of grasping force of the right finger f_{v1} followed the desired grasping force as a difference in results. Although there were differences between the grasping forces of the right finger f_{v1} and the left finger f_{v2}, it was natural that they differed, because the two opposite surfaces of the object were not parallel. Our simulation results showed that the proposed controller could simultaneously control the grasping force and the object's three coordinates.

VII. CONCLUSION

In this paper, we have introduced a two phased controller for a pair of 2-DOF soft fingers. This controller was capable of controlling an object's three coordinates. We also applied a grasping force controller to the proposed controller. In all simulations and experiments, the results successfully followed the desired trajectory, showing the validity of the proposed controller, both through simulations and experimentally. In the last section of this paper, however, we showed control only by simulating the manipulation of a trapezoidal prism. In assessing grasping force control with a real soft fingered hand, it is therefore necessary to develop a tactile sensor for these soft fingers.

REFERENCES

[1] Hanafusa, H. and Asada. H., "Stable Prehension by a Robot Hand with Elastic Fingers", *Proc. 7th Int. Symp. Industrial Robots*, pp.361–368, 1977.

[2] Hanafusa, H. and Asada. H., "A Robot Hand with Elastic Fingers and Its Application to Assembly Process", *IFAC Symp. Information and Control Problems in Manufacturing Technology*, pp.127–138, 1977.

[3] Paul, R. and Shimano, B., *Compliance and control*, Proc. on Joint Automatic Control Conference, pp.694–699, 1976.

[4] Mason, M. T., *Compliance and Force Control for Computer Controlled Manipulators*, IEEE Trans. SMC, SMC–11, No. 6, pp.418–432, 1981.

[5] Mason, M. T., *Compliant Motion*, Brady, M. *et al.* eds., *Robot Motion*, Cambridge, MIT press, pp.305–322, 1982.

[6] Hogan, N., *Impedance Control: An Approach to Manipulation*, ASME J. of Dynamic Systems, Measurement and Control, Vol. 107–1, pp.1–22, 1985.

[7] Cutkosky, M. and Kao, I., *Computing and controlling the compliance of a robotic hand*, IEEE Trans. Robotics and Automation, Vol. 5, No, 2, pp.151–165, 1989.

[8] Nevins, J. L. *et al.*, *Exploratory Research in Industrial Assembly Part Mating*, R-1276, The Charles Stark Draper Laboratory, Inc., 1980.

[9] Whitney, D. E., *Quasi-Static Assembly of Compliantly Supported Rigid Parts*, ASME J. of Dynamic Systems, Measurement and Control, Vol. 104, pp.65–77, 1982.

[10] Akella, P. and Cutkosky, M., *Manipulation with Soft Fingers: Modeling Contacts and Dynamics*, IEEE Int. Conf. Robotics and Automation, pp.764–769, 1989.

[11] Xydas, N. and Kao, I., *Modeling of contact mechanics and friction limit surfaces for soft fingers in robotics, with experimental results*, Int. Journal of Robotics Research, Vol. 18, No. 8, pp.941–950, 1999.

[12] Arimoto, S., Nguyen, P., Han, H. Y., and Doulgeri, Z., "Dynamics and control of a set of Dual Fingers with Soft Tips", *Robotica*, Vol. 18, pp.71–80, 2000.

[13] Doulgeri, Z., Fasoulas, H., and Ariomoto, S., "Feedback Control for Object Manipulations by a pair of Soft Tips", *Robotica*, Vol. 20, pp.1–11, 2002.

[14] Doulgeri, Z. and Fasoulas, H., "Grasping Control of Rolling Manipulation with Deformable Fingertips", *IEEE/ASME Trans. Mechatronics*, Vol. 22, No. 6, pp.1273–1279, 2006.

[15] Inoue, T. and Hirai, S., "Local Minimum of Elastic Potential Energy on Hemispherical Soft Fingertip", *IEEE Int. Conf, Robotics and Automation*, 2005.

[16] Inoue, T and Hirai, S., "Elastic Model of Deformable Fingertip for Soft-fingered Manipulation", IEEE Trans. on Robotics, Vol. 22, No. 6, pp.1273–1279, 2006.

[17] Inoue, T. and Hirai, S., "Mechanics and Control of Soft-fingered Manipulation", Springer–Verlag, ISBN 978-1-84800-980-6, January, 2009.

[18] Inoue, T. and Hirai, S., "A Two-Phased Object Orientation Controller on Soft Finger Operation", *IEEE/RSJ Int. Conf. Intelligent Robots and Systems*, 2007.

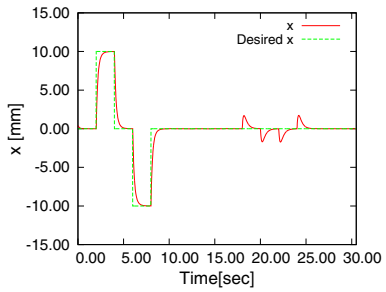

(a) x_{obj} vs. time

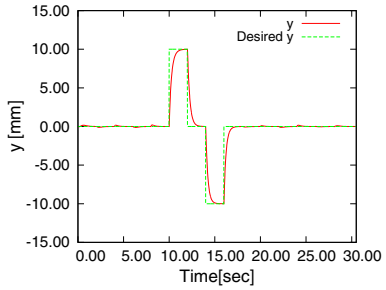

(b) y_{obj} vs. time

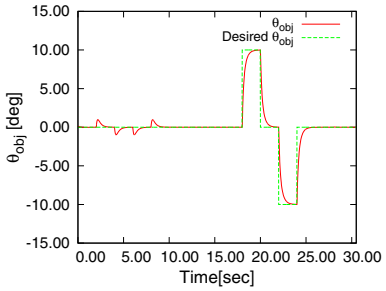

(c) θ_{obj} vs. time

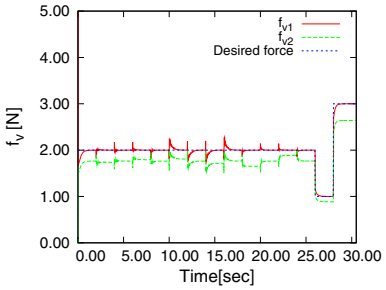

(d) f vs. time

Fig. 8. Simulation result of object force and object location control